European Radiology (2021) 31:8098–8107
https://doi.org/10.1007/s00330-021-07890-1

CARDIAC

Post-mortem CMR in a model of sudden death due to myocardial ischemia: validation with connexin-43

Giovanni Donato Aquaro[1] · Marco Di Paolo[2] · Benedetta Guidi[3] · Khatia Ghabisonia[4] · Angela Pucci[5] · Giacomo Aringheri[3] · Nikoloz Gorgodze[4] · Musetti Veronica[3] · Enrica Chiti[3] · Silvia Burchielli[1] · Emanuela Turillazzi[2] · Michele Emdin[1,4] · Davide Caramella[3] · Fabio A. Recchia[1,4]

Received: 17 January 2021 / Revised: 8 March 2021 / Accepted: 15 March 2021 / Published online: 20 April 2021

Abstract

Objectives We sought to evaluate the effectiveness of post-mortem cardiac magnetic resonance (PM-CMR) for the identification of myocardial ischemia as cause of sudden cardiac death (SCD) when the time interval between the onset of ischemia and SCD is ≤ 90 min.

Methods PM-CMR was performed in 8 hearts explanted from pigs with spontaneous death caused by occlusion of the left anterior descending coronary artery: 4 with SCD after ≤ 40 min of coronary occlusion and 4 between 40 and 90 min. PM-CMR included conventional T1 and T2-weighted image and T1, T2, and T2* mapping techniques. Imaging data were compared and validated with immunohistochemical evaluation of the altered proportion and redistribution of phosphorylated versus non-phosphorylated connexin 43 (CX43 and npCX43, respectively), an established molecular marker of myocardial ischemia.

Results At T2-weighted images, the ischemic core was hypointense (core/remote ratio 0.67 ± 0.11) and surrounded by and hyperintense border zone. Compared to remote myocardium, the ischemic core had higher T1 ($p = 0.0008$), and lower T2 ($p = 0.007$) and T2* ($p = 0.002$). Cytoplasmatic npX43 and the npCX43/CX43 ratio were significantly higher in animals deceased > 40 min than in others.

Conclusion PM-CMR can reliably detect early signs of myocardial damage induced by ischemia, based on conventional pulse sequences complemented by a novel ad hoc application of quantitative mapping techniques.

Key Points

- *Post-mortem MRI may help to understand cause of sudden cardiac death.*
- *Post-mortem MRI allows detection of signs of myocardial ischemia as cause of sudden cardiac death within 90 and 40 min following coronary occlusion as demonstrated in a pig model of myocardial ischemia.*
- *Signs of myocardial ischemia using conventional and mapping MRI technique are associated with the immunohistochemical changes of phosphorylated and dephosphorylated connexin-43 which is an established molecular marker of myocardial ischemia.*

Keywords Sudden cardiac death · Myocardial infarction · Magnetic resonance · Coronary artery disease

Giovanni Donato Aquaro and Marco Di Paolo contributed equally to this work.

✉ Giovanni Donato Aquaro
aquaro@ftgm.it

[1] Fondazione Toscana G. Monasterio, Via Giuseppe Moruzzi, 1, 56124 Pisa, Italy

[2] UO Medicina legale, University of Pisa, Pisa, Italy

[3] Clinical and Translational Science Research Department, University of Pisa, Pisa, Italy

[4] Institute of Life Sciences, Scuola Superiore Sant'Anna, Pisa, Italy

[5] Azienda Ospedaliero Universitaria Pisana, Pisa, Italy

Abbreviations

AMI	Acute myocardial infarction
CP	Cytoplasm
CX43	Phosphorylated connexin-43
FSE	Fast spin echo
ID	Intercalated disk
LCB	Lateral cellular border
LV	Left ventricle
MOLLI	Modified Lock-Locker
npCX43	Dephosphorylated connexin-43

PM-MRI	Post-mortem cardiac magnetic resonance
SCD	Sudden cardiac death
SSFP	Steady-state free precession

Introduction

Sudden cardiac death (SCD) is defined as the unexpected natural death from a cardiac cause within a short time period, generally ≤ 1 h from the onset of symptoms, in a person without any prior condition that would appear fatal [1]. Acute myocardial ischemia caused by partial or total occlusion of a coronary artery is the leading cause of malignant ventricular arrythmias and SCD in Western countries [2]. The autoptic evaluation based on traditional methods of organ examination is very challenging when SCD occurs within the first hours of ischemia, since cardiac lesions need more time to develop [3]. Acute myocardial infarction is usually unapparent on macroscopic examination if survival time after coronary occlusion is <12 h, while early histological markers such as hypereosinophilia, loss of cross striation, and wavy aspect of myocyte fibers, presumably due to changes in pH, myocardial water content, and disrupted calcium homeostasis appear no sooner than 4–6 h [4].

Customary histochemical staining procedures allow for detection of markers of acute myocardial ischemic damage only after 2 h of survival time [5]. Nonetheless, more recent techniques of immunostaining of the gap junction protein connexin-43 (CX43) seem to be able to identify the initial cardiomyocyte alterations caused by the ischemic insult [6]. In normal hearts, CX43 is phosphorylated and localized in the intercalated discs (ID), but insults such as ischemia, hypoxia, and hypothermia induce its dephosphorylation (npCX43) and redistribution of the npCX43 in the cytoplasm (CP) and lateral border (LCB) of cardiomyocytes [7, 8]. The increased npCX43/CX43 ratio at ID and in the CP and the drop of the respective CX43 levels is presently considered a reliable marker of myocardial ischemia [6]. Preliminary studies showed a good correlation between autoptic findings and post-mortem magnetic resonance (PM-MRI) in cases of acute, sub-acute, and chronic myocardial infarction [8–10]. Two different approaches were tested for PM-MRI scanning: whole-body or explanted hearts fixed in formalin.

In conventional T2-weighted images, acute ischemia/infarct is identifiable as a hypointense central core surrounded by a thin hyperintense border [11]. The hyperintense border, caused by edema and cellular reactions, progressively thickens during ischemia and, in the subacute phase, myocardial lesions appear diffusely hyperintense compared to remote myocardium. To date, no studies have tested the effectiveness of PM-MRI for the identification of myocardial ischemia as the cause of SCD within the first 90 min of coronary artery occlusion.

Moreover, T1, T2, and T2* mapping techniques, diffusely used in clinical MRI for the evaluation of myocardial tissue abnormalities, have not been exploited in PM-MRI to improve the evaluation of ischemic damage occurring within the first hours of coronary occlusion.

The aims of this study, performed in a pig model of myocardial infarction causing SCD, were as follows: (1) to compare the effectiveness of conventional and mapping PM-MRI techniques for the detection of myocardial markers of ischemic damage developing within 90 min of coronary artery occlusion; (2) to test possible correlations between PM-MRI and CX43/npCX43 alterations.

Material and methods

Cardiac arrest model

The hearts were obtained from pigs utilized in concomitant studies on experimental therapies for myocardial infarction. All the animals died before the randomization (treated vs controls) and did not receive any treatment. These protocols were compliant with the Guide for the Care and Use of Laboratory Animals published by the US National Institutes of Health (NIH Publication No. 85-23, revised 1996). The protocol for the animal studies (no. 76/2014 PR) was approved by the Italian Ministry of Health and was in accordance with the Italian law (D.lgs. 26/2014).

To induce myocardial infarction, male farm pigs (35–40 kg) were sedated with a cocktail of tiletamine hydrochloride (4 mg/kg, im) and zolazepam hydrochloride (4 mg/kg, im) and premedicated with atropine sulfate (0.1 mg/kg, im). General anesthesia was subsequently induced with propofol (2–4 mg/kg, iv) and maintained with 1–2% isoflurane in 60% air and 40% oxygen. After thoracotomy at the fifth intercostal space, the left anterior descending coronary artery was ligated below the second diagonal branch for 90 min, followed by reperfusion [12, 13].

During the 90 min of coronary artery occlusion, most pigs developed ventricular fibrillation treated with a standard resuscitation protocol, which included defibrillation. The resuscitation protocol included direct cardiac massage, with a frequency of 100/min. The massage was continuous during arrhythmia. Pigs were ventilated at a rate of 12 breaths per minute. The animals received open-chest epicardial defibrillations (40 J). Amiodarone (100 mg bolus iv) and adrenaline (0.1 mg/kg/iv) were administered between electrical discharges at 5-min intervals. Resuscitation maneuvers were attempted for 30 min after the start of ventricular fibrillation. After that time, cardiac arrest was considered irreversible, the heart was explanted, washed with physiological saline

solution, and fixed in 10% buffered formalin. The time elapsed between the start of coronary occlusion and the occurrence of ventricular fibrillation was recorded. Overall, 8 hearts from pigs that died within the first hour of coronary occlusion were included in the present study and divided into 2 groups: (1) death that occurred within the first 40 min (n = 4) and (2) death that occurred between 40 min and 1 h (n = 4).

The study on explanted hearts included two phases, first PM-MRI and then macroscopic examination, histopathological and immunochemical analyses of myocardial samples taken from the ischemic area and from the remote area.

PM-MRI

PM-MRI imaging was performed 7 days after heart fixation using a 1.5-Tesla magnetic resonance scanner (Signa HD CVi and Signa Artist, GE Healthcare) with a multichannel head-birdcage coil. The protocol included a whole-heart 3D steady-state free precession (SSFP) pulse sequence with the following parameters: FOV 200 mm, matrix 512 × 512, thickness 1 mm (interleaved to 0.3 mm), TR = 9 ms, TE = 4 ms, with a final voxel size of 0.3 × 0.3 × 0.3 mm. T1 mapping was performed using a modified Lock-Locker (MOLLI) pulse sequence with a 3(3)3(3)5 approach, acquired in short axis images using the following parameters: TE = 3 ms, thickness 4 mm, matrix 224 × 244. T2 mapping was performed using a multi-echo fast spin echo (FSE) pulse sequence in the same short axis views with the following parameters: thickness 4 mm, matrix 224 × 244. T2* mapping was performed using a multi-echo T2* pulse sequence, in the same short axis views, with the following parameters: thickness 4 mm, matrix 224 × 244. A MAGIC fingerprinting technique was also used to reconstruct a set of 20 images (FOV 200 mm, matrix 512 × 512, slice thickness 2 mm, no gap) of T1-weighted, T2-weighted, T2-STIR, and PD-weighted images in ventricular short axis views.

PM-MRI post-processing

Images were analyzed by two expert EACVI level III MRI accredited investigators. A dedicated cardiac post-processing software was used to analyze PM-MRI images. Left ventricular mass was measured by manually tracing endocardial and epicardial contours of the left ventricle [14]. Regional wall thickness was measured in all myocardial segments using the conventional AHA–ACC–ESC segmentation.

T1, T2, and T2* maps were generated and quantified for all myocardial segments. Myocardial signal intensity was expressed as arbitrary units, both in synthetic T1- and T2 -weighted images and in 3D-SSFP images.

Due to the high reproducibility of cardiac anatomical features among pigs, the occlusion of the left anterior descending artery after the second diagonal branch caused a constant involvement of the middle and apical anterior septum and, to a variable extent, the anterior wall. Therefore, we considered as the "core" of ischemia the middle and apical anterior septum, the "border zone" the immediate peri-ischemic surrounding area, and the "remote region" the opposite inferolateral wall, which served as control uninjured myocardium.

Macroscopic, histological, and immunohistochemical analyses

Data about macroscopic, histological, and immunohistochemical analyses are reported in supplemental material.

Statistical analysis

A semiquantitative evaluation of the immunohistochemical findings and gradation of the immunohistochemical reaction were expressed with an ordinal scale. The normal distribution was assessed by the Kolmogorov-Smirnov method. Normally distributed variables are expressed as mean ± SD, while median (25th–75th) was used for non-normally distributed variables. Data comparison was performed using ANOVA, the Kruskal-Wallis or Mann-Whitney test, as appropriate. A $p < 0.05$ was considered significant.

Results

PM-MRI and histological analyses were completed in 8 pig hearts, 4 with irreversible arrest occurring after ≤ 40 min and 4 between > 40 and 90 min of coronary occlusion. The average ischemic time was 42 ± 14 min. The characteristics of the 2 groups of animals with cardiac arrest are reported in Tables 1 and 2.

In all of the hearts, the ischemic area comprised the middle and apical anterior septum with a variable amount of anterior wall involvement. In all of them, the core ischemic region was hypointense in 3d-SSFP and in T2-weighted images. The hypointense core was surrounded by a thin hyperintense border zone that was more evident in hearts with an ischemic time > 40 min than in those with a shorter ischemic time. Examples of conventional T2-weighted image are showed in Fig. 1. The average extent of the hypointense core was 9.4 ± 4% of LV mass in the 8 hearts, whereas the surrounding hyperintense border zone was 5 ± 2%. In conventional T2-weighted images, the signal intensity of the ischemic core was lower than that of the remote myocardium, with the average signal intensity ratio core/remote of 0.67 ± 0.11. In contrast, the signal of the border zone was higher than core and remote myocardium. The average signal intensity ratio border zone/remote was 1.2 ± 0.08 and the ratio core/border zone was 0.55 ± 0.07. As shown in Table 2, the signal intensity ratio core/remote (0.76 ± 0.06 vs 0.58 ± 0.09, $p = 0.004$) and the ratio border/remote (1.28 ± 0.03 vs 1.15 ± 0.08, $p = 0.025$) were

Table 1 Score system for Cx43 and npCx43 semiquantitative evaluation

Score:	Cx43		npCx43	
	ID and anterior/lateral cell border (LCB)	Cytoplasm (CP)	ID and anterior/lateral cell border (LCB)	Cytoplasm (CP)
0	Not expressed	Not expressed	Not expressed	Not expressed
1	Thin linear or intermittent positivity	Scattered positivity	Thin linear or intermittent positivity	Scattered positivity
2	Dense but intermittent positivity	Patchy positivity	Dense but intermittent positivity	Patchy positivity
3	Dense band-like positivity	Diffuse positivity	Dense band-like positivity	Diffuse positivity

significantly higher in hearts that stopped beating after > 40 min of coronary occlusion than those with a lower ischemic time, demonstrating a trend towards increasing signal intensity in the ischemic core with the duration of ischemia.

T1, T2, and T2* values are showed in Fig. 2 and Table 2. T1 values were significantly higher in the core region than those in the remote myocardium in all the hearts from both groups ($p = 0.02$).

Table 2 Comparison between death at ischemia time ≤ and > 40 min

	Ischemia time ≤ 40 min	Ischemia time > 40–90 min	*p* value
Ischemic time (min)	28 ± 14	55 ± 10	
PM-MRI			
LV mass	62 ± 6	64 ± 8	0.83
Mid-septal wall thickness	10 (9–11)	12 (10–12)	0.18
Inferolateral wall thickness	11 (10–12)	12 (11–13)	0.23
T2w SI border/core	1.69 ± 0.1	2.1 ± 0.29	0.08
T2w SI core/remote	0.58 ± 0.09	0.76 ± 0.06	0.004
T2w SI border/remote	1.15 ± 0.08	1.28 ± 0.03	0.025
T1 core (ms)	444 ± 41	469 ± 141	0.75
T1 remote (ms)	276 ± 40	294 ± 26	0.46
T1 core/remote	1.51 ± 0.15	1.68 ± 0.28	0.34
T2 core (ms)	31 ± 3	37 + 3	0.03
T2 remote (ms)	53 ± 9	61 ± 9	0.17
T2 core/remote	0.58 ± 0.09	0.61 ± 0.02	0.90
T2* core (ms)	24 ± 5	31 ± 4	0.07
T2* remote (ms)	43 ± 3	45 ± 6	0.59
T2* core/remote	0.55 ± 0.08	0.69 ± 0.14	0.13
Immunohistochemistry			
ID CX43	1 (1–3)	1 (0–1)	0.06
LCB CX43	2 (1–3)	1 (0–1)	0.06
CP CX43	2 (1–3)	2 (2–3)	0.65
Total CX43	5 (4–7)	3 (2–4)	0.10
ΔLCB-ID CX43	0 (0–0)	0 (0.0)	
ΔCP-ID CX43	0 (−1–2)	1 (1–3)	0.18
ID npCX43	2 (1–2)	2 (1–2)	0.99
LCB npCX43	1 (1–2)	2 (1–2)	0.49
CP npCX43	1 (1–2)	3 (2–3)	0.039
Total npCX43	4 (3–5)	6 (5–6)	0.048
ΔLCB-ID npCX43	0 (−1–0)	0 (0–0)	0.32
ΔCP-ID npCX43	0 (−1–1)	1 (0–2)	0.17
npCX43 sum/CX43	0.6 (0.6–0.9)	1.8 (1.2–4)	0.04

PM-MRI, post-mortem cardiac magnetic imaging; *LV*, left ventricle; *T2w*, T2-weighted images; *ID*, intercalated disk; *LCB*, anterior-lateral cell border; *CP*, cytoplasm; *CX43*, connexin -43; *np-CX43*, non-phosphorylated CX43

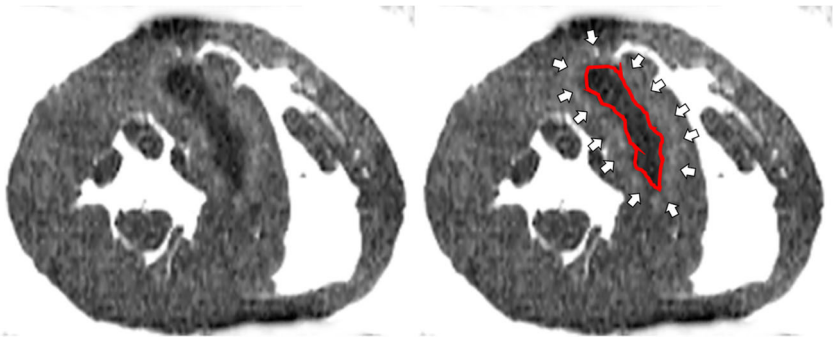

Fig. 1 Example of T2-weighted image of a pig heart that stopped beating after 30 min of coronary occlusion. It is possible to identify a hypointense core (red-bordered in right panel) and a thin border zone of hyperintensity (arrows). Of note, the signal generated by formalin, in which the heart was immersed, is not nulled by the rephasing pulse of fast spin echo

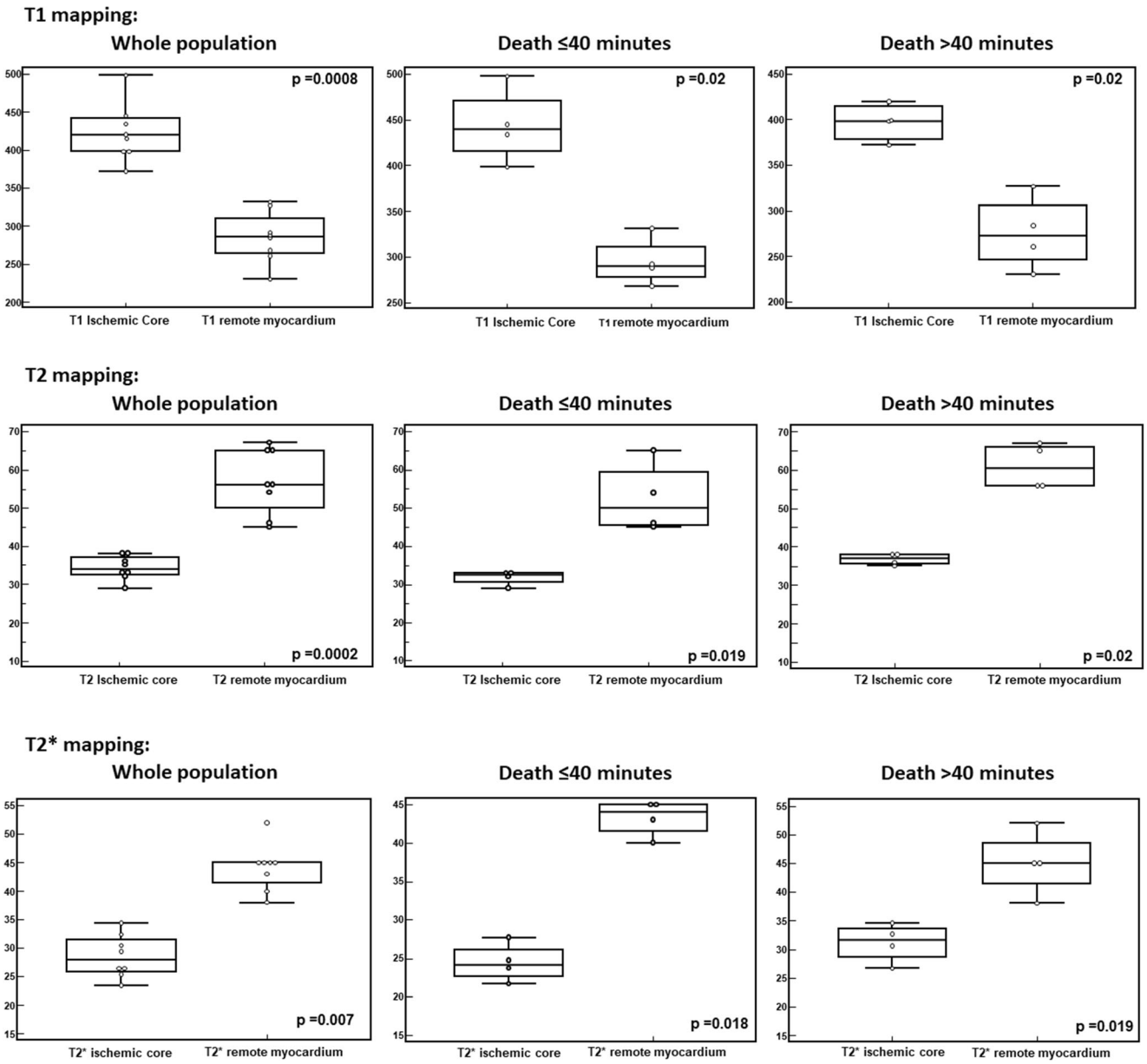

Fig. 2 T1, T2, and T2* mapping in the ischemic core and remote myocardium. In the ischemic core, T1 was significantly higher than in the remote myocardium, while T2 and T2* were significantly lower in the ischemic core than in the remote region. This pattern was found in both subgroups (death after ≤ 40 and > 40 min of coronary occlusion)

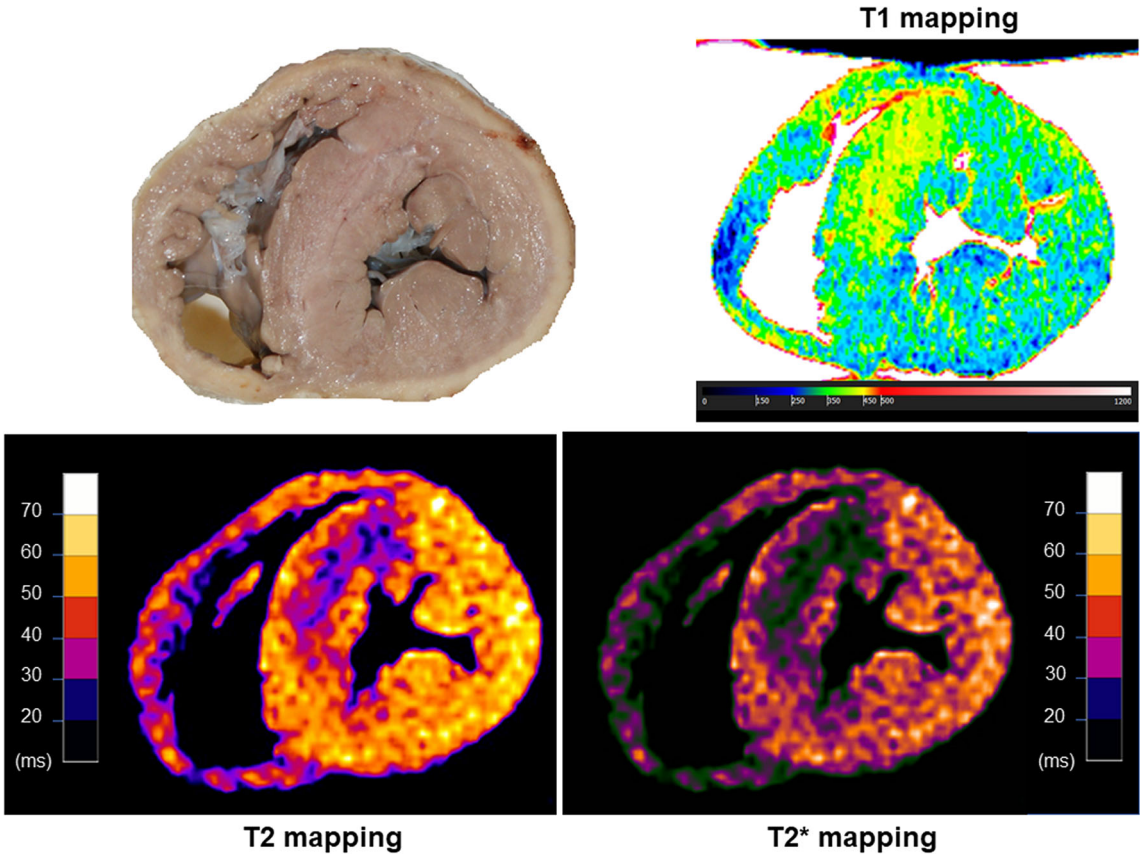

Fig. 3 T1, T2, and T2* maps: In this case, irreversible cardiac arrest occurred 55 min after coronary occlusion. An area of high T1 with low T2 and T2* is detectable in the anterior septum, corresponding to the ischemic core

In contrast, T2 and T2* values were significantly lower (Fig. 2) in the ischemic core than those in the remote myocardium. The T2 values of the ischemic core were higher in hearts that stopped beating after more than 40 min of coronary occlusion than in those with a shorter ischemic time (respectively, 31 ± 3 vs 37 ± 4 ms, $p = 0.03$). Examples of T1, T2, and T2* mapping images are showed in Fig. 3.

Histology and immunohistochemical analysis

Microscopic analysis revealed myofiber eosinophilia and foci of subendocardial contraction band necrosis in 4 hearts, whereas interstitial edema was detected in the anterior septum in 3 cases. An example of histological analysis is shown in Fig. 4. Table 3 and Fig. 5 report the results of the immunohistochemical analysis.

The dephosphorylation of CX43 in ischemic regions was proportional to the ischemia duration. Indeed, as shown in Table 2, a trend towards lower ID, CP, and LCB CX43 concentration, and a significantly higher CP npCX43 concentration was found in hearts that stopped after more than 40 min of coronary occlusion. The ratio between total npCX43 and CX4 was significantly lower in hearts that stopped after less than 40 min of coronary occlusion compared to others (respectively, median of npCX43/CX4 0.6, 25th–75th 0.6–0.9 vs 1.8 25th–75th 1.2–4, $p = 0.04$).

In the hearts that kept beating for more than 40 min during occlusion, total npCX43 was higher than total CX43 (respectively median of 6 (5-6) vs median of 3 (2-4), $p = 0.048$), whereas non-significant differences were found in hearts that stopped after ≤ 40 min of occlusion ($p = 0.13$).

Discussion

The main findings of this study are as follows: (1) in a pig model of VF/arrest occurring within the first 90 min of coronary artery occlusion, PM-MRI of explanted hearts was able to detect early tissue abnormalities as indicated by signal hypointensity in T2-weighted and SSFP images, increase of myocardial T1 and decrease of myocardial T2 and T2* in the ischemic core; (2) the ischemic core was surrounded by a thin hyperintense border zone of edema in T2-weighted images; (3) the immunohistochemical evaluation revealed a shift from phosphorylated to non-phosphorylated CX43 in hearts that stopped beating within the first 40 min of coronary occlusion, with more pronounced evidence after 1 h of occlusion.

Table 3 Semi-quantitative analysis of Cx43 and npCx43 immunopositivity

	ID score	LCB score	CP score	Total	ΔLCB-ID	ΔCP-ID
npCx43 ≤ 40 min						
Pig 1	1	1	2	4	0	1
Pig 2	1	1	1	3	0	0
Pig 3	2	1	1	4	−1	−1
Pig 4	2	2	1	5	0	−1
Cx43 ≤ 40 min						
Pig 1	1	1	3	5	0	2
Pig 2	1	1	2	4	0	1
Pig 3	3	3	2	8	0	−1
Pig 4	2	2	1	5	0	0
npCx43 > 40 min						
Pig 5	1	1	2	4	0	1
Pig 6	1	1	4	6	0	3
Pig 7	2	2	2	6	0	0
Pig 8	2	2	2	6	0	0
Cx43 > 40 min						
Pig 5	1	1	3	5	0	2
Pig 6	0	0	1	1	0	1
Pig 7	1	1	2	4	0	1
Pig 8	0	0	3	3	0	3

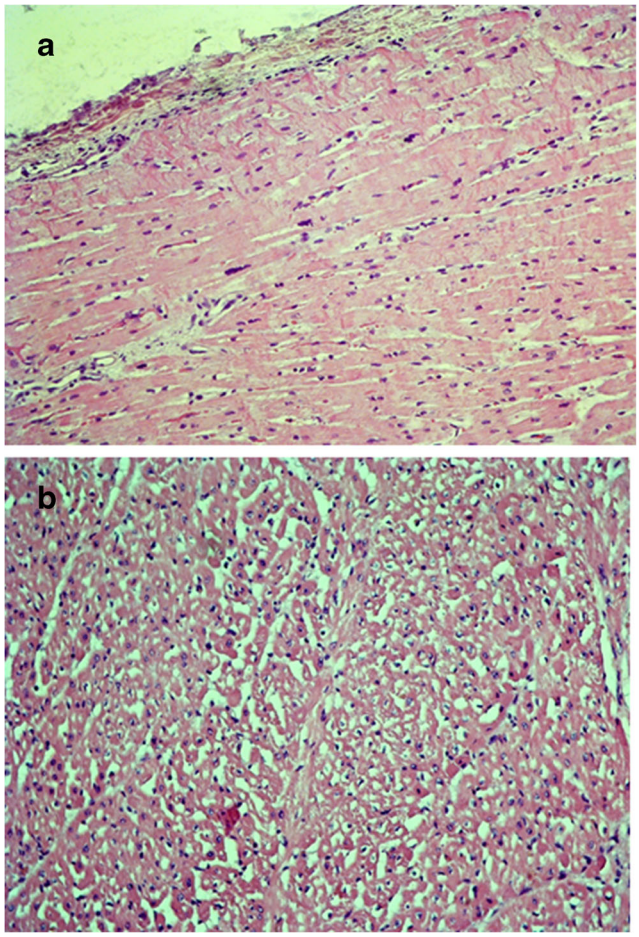

Fig. 4 Histological analysis on myocardial samples from hearts that stopped beating after 40 min of coronary occlusion, stained with hematoxylin and eosin: in panel **a**, subendocardial contraction band necrosis; in panel **b** interstitial edema (magnification × 10)

A similar experimental protocol was previously adopted by Ruder et al [11], who performed PM-MRI in a pig model of myocardial infarction, although, in their study, the heart was arrested after 120 min (60 min of coronary occlusion and 60 of reperfusion) and they used only a conventional, qualitative, MRI technique such as T2-weighted pulse sequence. Our model may be considered closer to real-life SCD and, importantly, we tested a novel application of mapping techniques, providing a quantitative assessment of myocardial abnormalities caused by ischemia.

Recently, Webb and coworkers performed PM-MRI with a 3-Tesla scanner in 8 hearts of pigs sacrificed within 3 h after ethanol-induced complete occlusion of the left anterior descending coronary artery [15]. The authors found a significant difference between ischemic and remote regions for T2 values, but not for T2*.

Our results suggest that PM-MRI is able to detect myocardial tissue abnormalities caused by ischemia also when death occurred within 40 min of coronary artery occlusion. Jachowski et al described the signs of ischemic injury using conventional T2-weighted images, consisting of a central core of intermediate/low signal intensity bordered by a rim of increased signal intensity [16]. Accordingly, in conventional T2-weighted and 3D-SSFP images of our pig hearts, we found the presence of a hypointense ischemic core surrounded by a hyperintense border zone. However, the most interesting results were derived from mapping techniques. T1 values remained significantly higher in the ischemic core than those in the remote myocardium, both when death occurred within 40 min of ischemia and both when it occurred between 40 and 90 min. Conversely, T2 and T2* values were lower in the ischemic core than in the remote myocardium. T1 usually increases in the presence of intracellular of interstitial edema, acute necrosis, or fibrosis, but in our pig hearts the ischemic time was obviously too short for the development of fibrosis, while edema was still absent in the core of lesion, as confirmed by the hypointense signal in T2-weighted images with low T2 values [17, 18]. However, this finding may be explained considering the effect of formalin that decreases significantly myocardial T1. We speculate that formalin permeated less effectively the ischemic core, thus maintaining a higher T1 in that region relative to the remote myocardium. On the other hand, the low T2 and T2* values found in the ischemic core were more predictable. Indeed, a low T2 corresponds to the hypointense signal at conventional T2-weighted

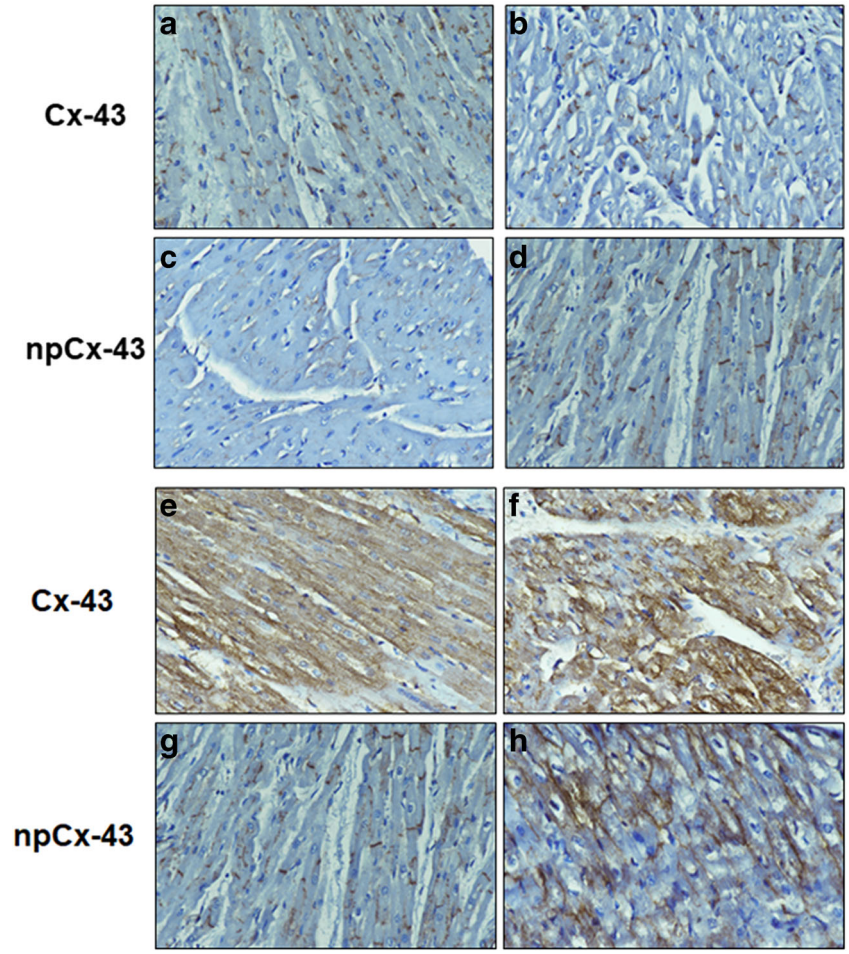

Fig. 5 Immunohistochemical assay of phosphorylated (CX-43) and dephosphorylated connexin-43 (npCX-43) in the ischemic region of hearts that stopped beating within 40 min of coronary occlusion (panels **a**–**d**) and between 40 and 90 min of coronary occlusion (panels **e**–**h**). In panels **a** and **c**, markers of ischemia are weak: CX-43 is mainly located in the intercalated disks and npCX-43 is almost absent. In panels **b** and **d**, the CX43 is less evident (**b**), whereas npCX43 is more evident in the intercalated disks. In the case with death between 40 and 90 min, signs of ischemia are more evident, with increased npCX43 and redistribution of CX43 from intercalated disks to lateral cell borders and cytoplasm. In panels **e** and **g**, CX43 is diffusely detectable in the cytoplasm and almost absent in intercalated disks (**e**), while npCX43 is found mostly at the level of intercalated disks (**g**). In panels **f** and **h**, CX43 is mostly found in the cytoplasm and in the lateral cell borders (**f**), while npCX43 is mostly located in lateral cell borders (magnification × 10)

images, reflecting the acute decrease of free-water content of the ischemic region caused by coronary occlusion. The low T2* could be explained by the decrease of free-water content, as well as T2. However, in in vivo MRI, a low T2* may also be associated with a decrease of blood oxygenation, due to the presence of deoxyhemoglobin with a change from ferric to ferrous state [9]. Moreover, hemorrhagic infarction could be another cause of low T2*, but it should have been associated with a similar drop of T1 which was instead increased in the ischemic core. However, at histology, we did not find any sign of intramyocardial hemorrhage.

By comparing hearts that stopped beating within the first 40 min with those with longer ischemic time, we could observe that the ratio of core/remote and border/remote signals in T2-weighted images was greater in those with a longer survival. These results demonstrated that the longer the ischemic time, the greater the probability to develop myocardial edema. In fact, the T2 value of the ischemic core was higher in hearts with a longer survival.

Another innovative aspect of our study was the validation of PM-MRI findings with immunohistochemical assessment of the altered CX43 to npCX43 ratio, which is considered an established marker of ischemic myocardial damage. We performed immunohistochemical analysis in pig hearts evaluating the fate of the phosphoprotein CX43, which is the gap junction forming monomer in human myocytes. Hypoxia induces dephosphorylation of CX43 into npCX43 and its redistribution from ID to the CP and LCB. Mark et al demonstrated that the phosphorylation state of Cx43 is reversibly regulated by specific mechanisms that are independent of hypoxia, but are tightly linked to cellular levels of ATP [12]. Beardslee et al induced global myocardial ischemia in isolated perfused rat hearts and found a progressive dephosphorylation of Cx43, accumulation of the npCX43 isoform within gap junctions, and translocation of Cx43 from gap junctions into an intracellular pool [6, 19]. We found that the npCX43/CX43 ratio was significantly higher in the pig hearts that stopped beating only after > 40 min of coronary occlusion. The npCX43/CX43 ratio increased from a median of 0.6 in those with shorter survival to a median of 1.8 in those with longer survival. In hearts explanted from the > 40 min group, total npCX43 was significantly higher than total CX43. Of note, PM-MRI T1, T2, and T2* values were found already abnormal in hearts that stopped after ≤ 40 min of occlusion, suggesting this imaging technique could be very sensitive to detect early myocardial changes associated with ischemia.

In our pig model, resuscitation maneuvers with DC shocks were attempted during ventricular fibrillation for 30 min before considering the cardiac arrest irreversible. Guensch et al demonstrated that five 200-J DC shocks of ventricular defibrillation increased both T1 and T2 in myocardial regions near the electric pad compared to remote areas [20]. However, we used a lower energy protocol (40 J) with an open-chest approach, by which the electric pads were placed over the basal anterior wall and RV free wall, therefore, not directly affecting the ischemic damage, that was seen mostly in the middle and distal anteroseptal region. Moreover, the changes of myocardial relaxation properties in our ischemic regions (increased T1, decreased T2 and T2*) were not consistent with the signs of DC shock damage reported by Guensch.

The formalin fixation implies a modification of myocardial relaxation times (supplemental data) but this is still an advantage of our method of PM-CMR because formalin allows keeping relatively constant relaxation times. The alternative approach, performing PM-CMR of the whole body, requires warming the frozen corpse to ambient temperature, but this cannot be ever guaranteed in internal tissue as the myocardium. This is a great limitation because relaxation times change with temperatures. Another possible approach is to perform PM-CMR of explanted heart without fixation in formalin, exposing the heart to air or embedding it in water. The main limitation of this further approach is that the PM-CMR should be performed immediately after explant in order to avoid the modification of relaxation times induced by post-mortem phenomena.

Limitations

This was a methodological study with a small population of pigs and further studies are needed to confirm the effectiveness of PM-MRI to evaluate ischemia as cause of sudden death in humans.

Our pig model of ischemia cannot reflect all the scenarios of SCD caused by myocardial ischemia. In particular, SCD in patients with previous PCI or myocardial infarction could present with different tissue abnormalities that are absent in our model. However, in such cases, the clinical history of the patients is very helpful for the final forensic diagnosis. Our model matches better with ischemic SCD in patients without a previous history of CAD, where the final forensic diagnosis is more challenging.

The hyperintense border zone detected with conventional T2-weighted images was too thin for measuring T1, T2, and T2*, due to the lower spatial resolution of the mapping technique compared to conventional images and 3D-SSFP.

In this study, we performed a transitory occlusion of coronary artery (90 min) and we could not evaluate the capability of PM-MRI to detect coronary artery anatomy. Indeed, PM-MRI might be able to detect coronary artery stenosis, increasing its effectiveness to detect ischemic heart disease

Conclusions

The results of our study demonstrate, for the first time, that PM-MRI might be used to identify ischemia as a cause of SCD occurring within the first 90 min of coronary occlusion.

Supplementary Information The online version contains supplementary material available at https://doi.org/10.1007/s00330-021-07890-1.

Funding This study has received funding by the Italian Ministry of Health grant RF-2011-02348164 "CardioRigen" (FAR).

Declarations

Guarantor The scientific guarantor of this publication is Giovanni Donato Aquaro.

Conflict of interest The authors of this manuscript declare no relationships with any companies whose products or services may be related to the subject matter of the article.

Statistics and biometry Giovanni Donato Aquaro kindly provided statistical advice for this manuscript.

Informed consent Approval from the institutional animal care committee was obtained.

Ethical approval Institutional Review Board approval was obtained.

Methodology
- prospective
- experimental
- performed at one institution

References

1. Myerburg RJ, Castellanos A (1997) Cardiac arrest and sudden death. In: Braunwald E (ed) Heart disease: a textbook of cardiovascular medicine. WB Saunders, pp 742–779
2. Benjamin EJ, Blaha MJ, Chiuve SE et al (2017) Heart disease and stroke statistics–2017 update: a report from the American Heart Association. Circulation 135:e146–e603
3. Brinkmann B, Sepulchre M, Fechner G (1993) The application of selected histochemical and immunohistochemical markers and procedures to the diagnosis of early myocardial damage. Int J Leg Med 106:135–141
4. Ortmann C, Pfeiffer H, Brinkmann B (2000) A comparative study on the immunohistochemical detection of early myocardial damage. Int J Leg Med 113:215–220
5. Turillazzi E, Di Paolo M, Neri M, Riezzo I, Fineschi V (2014) A theoretical timeline for myocardial infarction: immunohistochemical evaluation and western blot quantification for interleukin-15 and

monocyte chemotactic protein-1 as very early markers. J Transl Med 12:188
6. Kawamoto O, Tomomi M, Ishikawa T, Hitoshi M (2014) Immunohistochemistry of connexin 43 and zonula occludens-1 in the myocardium as markers of early ischemia in autopsy material. Histol Histopathol 29:767–775
7. Hesketh GG, Shah MH, Halperin VL et al (2010) Ultrastructure and regulation of lateralized connexin43 in the failing heart. Circ Res 106:1153–1163
8. Beardslee MA, Lerner DL, Tadros PN et al (2000) Dephosphorylation and intracellular redistribution of ventricular connexin43 during electrical uncoupling induced by ischemia. Circ Res 87:656–662
9. Guidi B, Aquaro GD, Gesi M, Emdin M, Di Paolo M (2018) Postmortem cardiac magnetic resonance in sudden cardiac death. Heart Fail Rev 23:651–665
10. Di Bella G, Siciliano V, Aquaro GD et al (2013) Scar extent, left ventricular end-diastolic volume, and wall motion abnormalities identify high-risk patients with previous myocardial infarction: a multiparametric approach for prognostic stratification. Eur Heart J 34:104–111
11. Ruder TD, Ebert LC, Khattab AA, Rieben R, Thali MJ, Kamat P (2013) Edema is a sign of early acute myocardial infarction on postmortem magnetic resonance imaging. Forensic Sci Med Pathol 9: 501–505
12. Gabisonia K, Prosdocimo G, Aquaro GD (2019) MicroRNA therapy stimulates uncontrolled cardiac repair after myocardial infarction in pigs. Nature 569:418–422
13. Lionetti V, Aquaro GD, Simioniuc A (2009) Severe mechanical dyssynchrony causes regional hibernation-like changes in pigs with nonischemic heart failure. J Card Fail 15:920–928
14. Aquaro GD, Camastra G, Monti L et al (2017) Working Group "Applicazioni della Risonanza Magnetica" of the Italian Society of Cardiology. Reference values of cardiac volumes, dimensions, and new functional parameters by MR: a multicenter, multivendor study. J Magn Reson Imaging 45:1055–1067
15. Webb B, Manninger M, Leoni M et al (2020) T2 and T2∗ Mapping in ex situ porcine myocardium: myocardial intravariability, temporal stability and the effects of complete coronary occlusion. Int J Leg Med 134:679–690
16. Jackowski C, Warntjes MJ, Berge J, Bar W, Persson A (2011) Magnetic resonance imaging goes postmortem: noninvasive detection and assessment of myocardial infarction by postmortem MRI. Eur Radiol 21:70–78
17. Haaf P, Garg P, Messroghli DR, Broadbent DA, Greenwood JP, Plein S (2016) Cardiac T1 mapping and extracellular volume (ECV) in clinical practice: a comprehensive review. J Cardiovasc Magn Reson 18:89
18. Messroghli DR, Moon JC, Ferreira VM et al (2017) Clinical recommendations for cardiovascular magnetic resonance mapping of T1, T2, T2* and extracellular volume: a consensus statement by the Society for Cardiovascular Magnetic Resonance (SCMR) endorsed by the European Association for Cardiovascular Imaging (EACVI). J Cardiovasc Magn Reson 19:75
19. Ahn JW, Huh GY (2015) The efficacy of connexin 43 expression in the myocardium as an early ischemic marker in forensic autopsy. Korean J Leg Med 39:6–11
20. Guensch DP, Yu J, Nadeshalingam G, Fischer K, Shearer J, Friedrich MG (2016) Evidence for acute myocardial and skeletal muscle injury after serial transthoracic shocks in healthy swine. PLoS One 11:e0162245